doi:10.2533/chimia.2015.284 Chimia 69 (2015) 284–289

Inkjet Printing Meets Electrochemical Energy Conversion

Andreas Lesch, Fernando Cortés-Salazar, Victor Costa Bassetto, Véronique Amstutz, and Hubert H. Girault*

Abstract: Inkjet printing is a very powerful digital and mask-less microfabrication technique that has attracted the attention of several research groups working on electrochemical energy conversion concepts. In this short review, an overview is given about recent efforts to employ inkjet printing for the search of new electrocatalyst materials and for the preparation of catalyst layers for polymer electrolyte membrane fuel cell applications. Recent approaches of the Laboratory of Physical and Analytical Electrochemistry (LEPA) at the École Polytechnique Fédérale de Lausanne for the inkjet printing of catalyst layers and membrane electrode assemblies are presented and future energy research directions of LEPA based on inkjet printing in the new Energypolis campus in the Canton of Valais are summarized.

Keywords: Catalyst layers · Electrocatalysts · Electrode fabrication · Energy conversion · Inkjet printing

1. Introduction

Inkjet printing is by now a ubiquitous microfabrication technique for depositing a wide range of materials that can be used in electrochemistry to functionalize electrodes.[1–3] It is a fast and flexible technique operating at relatively low cost and can be scaled up to the industrial level, for instance by increasing the number of nozzles in the printheads. In printed electronics, an inkjet printer is generally considered as a 2D microfabrication device, but the third dimension can be achieved by multi-layer printing. Various post-processing techniques, such as thermal curing or UV photopolymerization, transform the ink into a functional, mostly solid material. Inkjet printing has been used for instance to fabricate organic thin film transistors (OTFTs), organic light emitting diodes (OLEDs), solar cells, supercapacitors, sensing devices and biomaterials.[3–6] Nowadays, it is used in many research laboratories and it is approaching the industrial production level.

The diversity of printable materials as well as the flexibility in the process design makes inkjet printing also interesting for energy research, in particular for the fabrication of electrochemical energy storage and conversion devices including batteries and fuel cells. In such devices, electrical energy can be stored and released reversibly as chemical energy by electrochemical oxidation or reduction processes. The underlying reactions take place at so-called catalyst layers (CLs) that are composed of materials favoring the desired electrochemical reactions by increasing their rate. Many efforts are made to develop reliable electrochemical energy storage systems, such as rechargeable batteries, redox flow batteries and electrochemical supercapacitors, and electrochemical conversion devices, such as polymer electrolyte membrane fuel cells (PEMFCs), solid oxide fuel cells, electrolysers or photoelectrochemical cells that are composed of several functional layers including the CLs. The fabrication of these devices requires accuracy, reliability and reproducibility at low cost, which can principally be provided by inkjet printing.

In this short review, recent inkjet printing approaches related to electrochemical energy conversion systems with focus on combinatorial catalyst libraries and CLs for PEMFCs are presented. In addition, some of the recent and future research activities of LEPA at the new Energypolis campus in the Canton of Valais based on inkjet printing for electrochemical energy conversion devices are introduced.

*Correspondence: Prof. Dr. H. H. Girault
Laboratoire d'Electrochimie Physique et Analytique
EPFL-Valais
Rue de l'Industrie 17, CH-1950 Sion
Tel.: +41 21 693 31 51
E-mail: hubert.girault@epfl.ch

2. Inkjet Printing

2.1 *Technical Principles*

For inkjet printing, stable and reproducible droplets need to be generated at jetting frequencies ranging from several Hz to kHz. Two types of inkjet printing technologies have been introduced for droplet generation, *i.e.* continuous inkjet (CIJ) and drop-on-demand (DOD) inkjet (Fig. 1).[7]

In CIJ, which is usually employed in the packaging and labeling industry due to its relative high operation speed, slightly charged ink droplets are constantly created from a biased nozzle. The continuous stream of droplets can be interrupted by deflecting the charged droplets applying an external electric field and catching the droplets in a collector. In principle, the collected ink can be used for refilling, but this could lead to ink contamination, which is critical in material science. This results in a relative large amount of ink waste while another disadvantage is the requirement for electrically chargeable inks. Such limitations are irrelevant for DOD printers where droplets are generated only when requested. For these reasons, DOD inkjet printing became attractive for material deposition and in the following the focus is only on this inkjet printing mode. In DOD systems, a pressure pulse is generated by thermal, piezoelectric or electrostatic actuation leading to the ejection of a droplet from a small chamber located in the printhead and filled with the ink. The released ink volume is compensated by a refill from the ink reservoir at the back of the printhead. In thermal DOD printers, the evaporation of the solvent of the ink induced by a heated resistor generates the

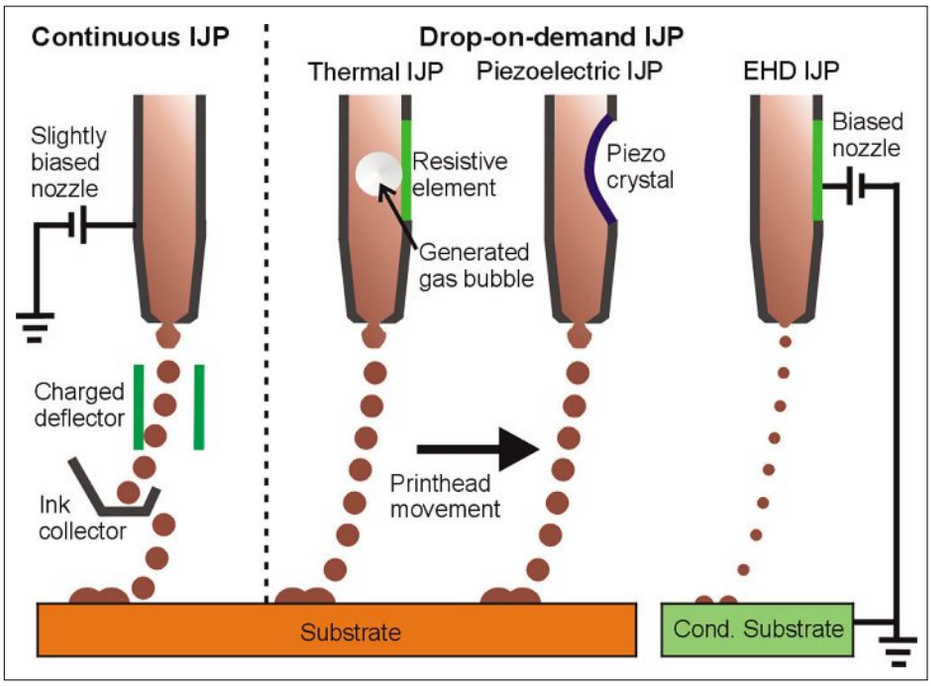

Fig. 1. Continuous *vs*. drop-on-demand inkjet printing.

pressure pulse. In piezoelectric based systems, this is realized by a mechanical distortion of the piezoelectric material due to an applied voltage pulse. One alternative is electrohydrodynamic (EHD) inkjet printing where an electrode is located inside the ink chamber while a conductive substrate is used as the counter electrode.[8,9] An electric field is applied and charged species in the ink accumulate at the meniscus–air interface. At a certain point, the electrostatic pressure becomes so large that it overcomes the surface tension resulting in droplet formation. The resolution of such a system is less dependent on the nozzle size and can lead even to nanometer sized surface features, but the substrate needs to be conductive.[10,11] In thermal inkjet printing, the ink has to be vaporized and resist at the same time the high temperatures; hence, it can only be operated with aqueous inks. Printheads for EHD require inks with charged particles. Therefore, piezoelectrically driven systems represent the most widely used printhead for material deposition since they show the largest flexibility for ink properties and droplet generation. Depending on the manufacturer, nominal droplet volumes can range between 1 and 80 pL and the number of addressable nozzles can be between 1 and 1024.

2.2 *Ink Property Requirements and Droplet/Substrate Interaction*

In order to generate stable droplets, which is essential for printing highly resolved patterns, inkjet inks need to fulfill certain requirements in terms of physical properties and fluid dynamics. Depending on the different commercial and custom-made jetting concepts, those ink requirements can vary significantly. The most important characteristics for droplet generation, ink–substrate interaction and post processing techniques are summarized in the following, and more details can be found in recent reviews.[12,13] The viscosity and surface tension of the ink need to be within certain ranges (*e.g.* 10–12 mPa s and 28–42 mN m^{-1}) because they influence the droplet formation and stability. For instance, a too high value for the surface tension can lead to split and satellite droplets rather than resulting in a stable jetting. On the other hand, lowering the surface tension too much can result in a leakage of the ink from the nozzle or in covering of the entire nozzle orifice making jetting impossible. The droplet formation is caused by mechanic waves in the printhead and proper viscosities support droplet stabilization due to a damping effect. Most inkjet inks are Newtonian liquids and the viscosity is stable at most obtained shear rates, but can be lowered for instance by increasing the ink temperature during printing. Generally, the interplay of both the surface tension and the viscosity defines the regime of ink printability among other parameters such as the droplet velocity. In order to adjust the surface tension and viscosity, solvents, polymers and surfactants can be added to the ink. But it has to be taken into consideration that additional components in the ink need to be removed during post processing and that the functionality of the desired patterns can be affected. Moreover, when printing nanoparticle (NP) dispersions the situation becomes more complex.[3] Generally, NPs should be 100 times smaller than the nozzle orifice diameter (*i.e.* 200 nm for a 20 μm nozzle). Usually, NPs tend to form aggregates that have to be broken mechanically by milling or ultrasound-based processes, which is by itself a challenging process. Hence, large aggregates can resist such treatment and even when small enough they can easily aggregate again or precipitate blocking the nozzles and preventing printing. Therefore, such large particle aggregates have to be removed by filtering or centrifugation, and an appreciable amount of the raw material can get lost. This becomes important in particular for expensive electrocatalysts based on precious metals. As a consequence, many efforts are made to suspend NPs by chemical modification of their surface or by the addition of surfactants or other species.[3] However, such additives can affect some properties of the printed film. For instance, it can lower its electrical conductivity, which requires the deposition of more layers or harsh post processing operations (*e.g.* high temperature treatments) to compensate for such an effect. One alternative approach to overcome NP aggregation is to print highly soluble precursors from which the desired NPs are synthesized directly on the surface after the printing process (*vide infra*).

Once an ink fulfills the requirements for the applied printhead, the formation of droplets depends on the applied actuation signal (for piezo-driven printheads: the voltage profile and amplitude), the jetting frequency and the distance between nozzles and substrate. Such parameters need to be optimized to obtain stable and reproducible droplets. Deviated and satellite droplets have to be avoided because they reduce significantly the printing resolution.

Another challenge is the drop–substrate interaction, which depends on the physicochemical properties of the ink as well as of the substrate.[12] The wetting of the substrate and the formation of a flat droplet on a surface after impact depend on several factors including inertial and capillary forces. Typically, on the very short time scale a drop diameter oscillation occurs, while capillary forces become dominant at longer times until equilibrium is achieved. The final droplet shape can be characterized by the contact angle between the substrate and drop surfaces and depend basically on the surface energy of the substrate and the surface tension and drying behavior of the ink. In order to generate continuous patterns, such as lines and rectangles, adjacent ink droplets need to overlap on the surface. Besides the importance of defining a proper drop spacing that influences the merging of interacting droplets, the deposited ink should not flow over the surface, as it would lead to the formation of bigger droplets due to poor attach-

ment and coalescence. This will certainly result in inhomogeneous, less resolved and partially disconnected patterns.

Finally, the ink has to be transformed into its desired phase by thermal or photochemical means. During drying of the ink the so-called coffee stain effect can be an issue.[14] Indeed, during solvent evaporation the ink solvent flows from the center of the droplet to the contact line accumulating particles at the rim of the printed structure, which after precipitation appear as a coffee ring of more concentrated particles. Many efforts are made to reduce this effect, for instance, by adjusting the substrate temperature and porosity, formulating solvent mixtures with different vapor pressures or inducing phase changes by gel formation.[15,16]

3. Inkjet Printing of Electrocatalysts and Catalyst Layers

Inkjet printing has been employed in two ways for energy research that will be discussed thoroughly in this chapter. On the one hand it can be used to identify new catalyst composites by generating combinatorial catalyst libraries applying parallel printheads that can deposit a wide range of catalytic materials. On the other hand, once a suitable catalyst has been identified, it can be used to create CLs of well-defined features for energy conversion.

3.1 *Inkjet Printing of Electrocatalysts*

The possibility to deposit electrocatalysts and combinatorial libraries of electrocatalysts in a high throughput manner by inkjet printing is of high value, because the catalytic activity of new mono and multicomponent systems is difficult to predict theoretically. The approach becomes very powerful when several printheads are used in parallel with separated ink reservoirs filled with different materials. Since the catalyst composite is formed after deposition, the inks need to contain catalyst precursors. Each jetted ink droplet has a known composition and by controlling the number of droplets from the different inks, arrays of catalyst spots with gradient compositions can easily be prepared. After post-processing, the catalytically most active composition can be identified by using different screening methods including fluorescence,[17] employing electrode arrays,[18,19] scanning electrochemical microscopy[20,21] and electrochemical scanning droplet cells.[22]

Inkjet printed electrocatalyst libraries were reported first by Reddington *et al.* who printed Pt, Ru, Os and Ir based halide salts.[17] Subsequently, quaternary Pt–Ru–Os–Ir compositions were synthesized by chemical reduction with borohydride. A significant increase in catalytic activity was found as anode catalyst in direct methanol fuel cells by the addition of small amounts of Os and Ir, a result that was obtained thanks to the high-throughput fabrication by inkjet printing. The printing concept was also employed by Bard and co-workers who prepared electrocatalyst libraries of Pt and Ru for the oxygen reduction reaction.[23] Later, the authors prepared binary mixtures of Co and Cu with Pd, Ag and Au by reducing the inkjet printed salts with hydrogen.[20] More recently, Seley *et al*. printed combinatorial libraries of rare earth metals such as Ir, Pt, Pd and Rh by pyrolysis in air in order to improve the performance of IrO_2-based water electrolysis catalysts.[24]

Currently, many efforts are made to replace precious metals such as Pt and Ir as electrocatalysts in energy conversion systems by low cost materials that meet or exceed the catalytic properties of the established systems. In this respect, inkjet printing provides a powerful fabrication tool to look for promising alternatives. Such inkjet printed materials could be metal oxides as recently reviewed by Liu *et al*.[25] Parkinson and co-workers formulated inks that contain mainly metal nitrates that were thermally converted into oxides at 500 °C.[26–30] Several multi metal oxide patterns were created to find very active photoelectrocatalysts for water splitting, such as Bi–V–W-based oxides with specific stoichiometric composition.[29] The concept of pyrolyzing metal nitrates has also been employed by Katz *et al.* who optimized the solubility of some metal salts by adjusting the pH of the aqueous ink solutions to acidic or neutral, respectively.[31]

The potential of the high-throughput multi-component deposition by inkjet printing has been demonstrated by Liu *et al*.[32] Several metal salts based on nitrate, chloride, acetate, alkoxide and silicate were applied in parallel using colloidal nanoparticle dispersions in amphoteric non-aqueous solvents (Fig. 2a). Combinatorial libraries of up to eight component mesoporous metal oxides for the photocatalytic hydrogen evolution reaction were obtained with a modified printer at a rate of 1,000,000 formulations h^{-1}. Besides the metal oxide precursors the inks contained structure-directing agents and the pH of the ink was well adjusted. After printing, the patterns were calcined at 350 °C. This printing system found several further applications, for instance for screening the catalytic activity of several multi-component oxides for the oxygen evolution reaction (OER)[22,33–35] (Fig. 2b) and also to prepare libraries for the study of the bubble formation at (Ni–Fe–Co)O_x OER catalysts.[36]

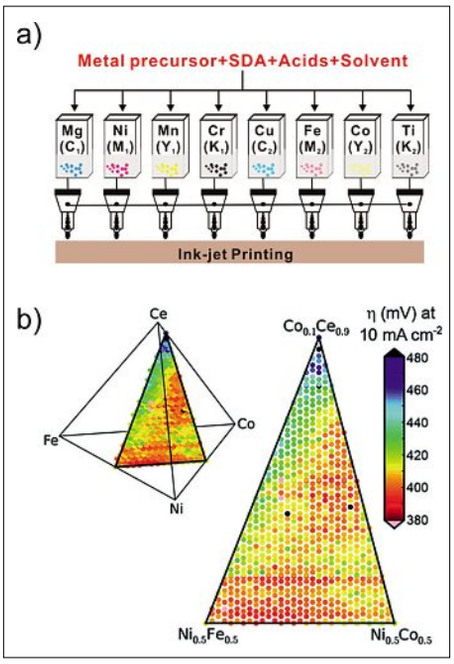

Fig. 2. a) Schematic representation of parallel inkjet printing of various metal precursor inks in non-aqueous solvents with structure-directing agents (SDA) and acids to create combinatorial libraries of multicomponent mesoporous metal oxides. Reprinted with permission from *Nano Letters* **2012**, *12*, 5733-5739. Copyright 2012 American Chemical Society. b) Electrocatalytic performance for the oxygen evolution reaction of inkjet printed quaternary (Ni–Fe–Co–Ce) oxides. Reproduced from *Energy Environ. Sci.* **2014**, *7*, 682–688 with permission of The Royal Society of Chemistry.

One advantage of printing metal salts is certainly the big range of precursor salts that can be applied and lead to combinatorial libraries composed of a huge variety of metal-composite oxides. A disadvantage is that often harsh post treatment procedures are required limiting the choice of substrates and ink additives.

3.2 *Inkjet Printing of Catalyst Layers*

In PEMFCs, oxygen and hydrogen are converted into water and electrical energy at two CLs locally separated by a polymer electrolyte membrane (PEM). A CL represents a three-dimensional network composed typically of the electrocatalyst (*e.g.* Pt) supported on an electron-conducting phase (*e.g.* carbon black; solid phase), a binder and/or an ionic conducting phase (for the proton transport; liquid phase) and pores for the transport of gaseous reactants and products (hydrogen, oxygen and water, respectively; gaseous phase). These phases need to form a three-phase boundary where the electrochemical reactions occur. The exact composition, fabrication and the properties of the CL are critical for the device performance and stability. In fact, one challenge is to prepare reproducibly

highly active and stable CLs (*i.e.* high catalyst loading, good electronic conductivity, good mass transport of reactants and products and high stability) either by depositing the CL on the membrane (catalyst-coated membrane – CCM) or on the gas diffusion layer (catalyst-coated gas diffusion layer – CCG). Conventional preparation methods include spraying, painting and screen-printing. More recent approaches employ for instance sputtering deposition and electro-spray deposition, but also inkjet printing in order to reduce the Pt loading and to increase at the same time the Pt utilization. Membrane electrode assemblies (MEAs) are then usually obtained by hot pressing of an anode, electrolyte membrane (usually Nafion) and a cathode.

Taylor *et al.* developed several inks based on various commercial and self-made Pt catalyst NPs supported on various carbon black materials and used thermal inkjet printing to print a CL onto a carbon cloth acting as the gas diffusion layer (GDL).[37] Catalyst loadings as low as 0.021 mg Pt cm^{-2} and a high Pt utilization of 17.6 kW g^{-1} Pt were achieved. The authors have also demonstrated the flexibility of inkjet printing as they printed CLs composed of graded Pt concentrations starting from high at the Nafion membrane (*i.e.* 50 wt% Pt) to low at the GDL (*i.e.* 10 wt% Pt). Towne *et al.* formulated an ink with Pt/C aggregates smaller than 2 µm that could be used with piezo as well as thermal inkjet printers.[38] MEAs were prepared by depositing the ink onto a commercial Nafion membrane and catalyst loadings of 0.2 mg Pt cm^{-2} could be achieved. The authors demonstrated the importance of the removal of ink components with high boiling points such as ethylene glycol, which was used to adjust the ink viscosity. The tested CLs showed a similar performance compared to commercial MEAs. Inkjet printing has also been used by several groups to prepare and optimize CLs of low catalyst loadings. Saha *et al.* achieved ultra-low Pt loadings (0.02-0.12 mg cm^{-2}) by printing few layers of catalyst ink on a Nafion membrane.[39] Recently, Shukla *et al.* followed this strategy to obtain 0.026 mg Pt cm^{-2} CLs and analyze the influence of a varying Nafion content in the ink to determine the limiting effects of the MEA performance.[40] It was found that between 20–40 wt% Nafion content the macro-scale transport of oxygen and protons is not limiting the function of the inkjet printed MEA. Furthermore, the authors reported an increase of the Pt utilization from 12.4 to 47.6 kW g^{-1} Pt by increasing the operating oxygen gauge pressure from ambient conditions to 2 bar. Yazdanpour *et al.* investigated the effect of hot pressing on the performance of Nafion membranes decorated with a CL of carbon nanotubes supported Pt and Nafion through thermal inkjet printing of the catalyst containing ink either directly onto the Nafion membrane or onto a Teflon substrate for subsequent decal transfer.[42] The authors reported that their CCM fabricated MEAs gave the highest power density (*i.e.* a peak power density of 231.54 mW cm^{-2}) when hot-pressed for 3 min at 800 psi and 100 °C. Wang *et al.* employed inkjet printing for impregnating Nafion-free Pt/C based CLs on carbon paper with Nafion containing inks.[42] The results were compared with spray coating and it was found that the inkjet printing method resulted in higher catalyst utilization with the same Nafion loading.

LEPA has recently started to implement inkjet printing for several microfabrication processes that have been realized in the past by photolithographic techniques or screen-printing. For instance, inkjet printing is used to produce with high accuracy and reproducibility batches of amperometric antioxidant sensors based on carbon nanotubes and nano-hydrogels.[43,44] Micro-3D-patterns and test samples for scanning electrochemical microscopy and electrostatic spray ionization mass-spectrometry imaging have been prepared as well.[45,46] Furthermore, inkjet printing has been employed in LEPA to create CLs and MEAs for PEMFCs. Similar to the works reported by the groups of Taylor,[37] Towne,[38] Karan[39] and Secanell[40] stable ink formulations of Pt/C inks with Nafion (Fig. 3a) were generated based on DI water and isopropanol, avoiding the addition of solvents with high boiling temperatures. The inks could be jetted with high reproducibility and accuracy using up to 16 consecutive nozzles as shown for six exemplary nozzles in Fig. 3b. The amount of material deposited depends on the printing parameters such as the number of inkjet printed layers (IJPLs). Fig. 3c shows CLs printed on Nafion NR-212 with 1, 6, 9 and 20 IJPLs. Even with one printed layer, the CL can clearly be identified by eye. As analyzed by energy dispersive X-ray fluorescence microscopy, the Pt loading with 30 IJPLs of the Pt/C-Nafion ink is 0.04 mg Pt cm^{-2}. It can be increased by multiplying the number of IJPLs. Indeed, commercial MEAs contain about 0.4 mg Pt cm^{-2}. After immersing the inkjet printed CLs for 12 h in 60 °C heated water, it could be confirmed that the CLs were stable and well attached to the membrane (Fig. 3d). Inkjet printing of CLs provides indeed a high resolution patterning tool as can be seen by the features printed in Fig. 3e and f. Finally, a complete MEA was generated by printing two CLs (5.4 cm × 5.4 cm and each with 0.04 mg Pt cm^{-2}) on both sides of a Nafion NR-212 membrane (Fig. 3g).

The electroactive surface area determined by CO stripping was 12 cm^2 Pt cm^{-2}, which is more than ten times lower than commercial MEAs due to the low Pt loading observed. Polarization curves of the MEA were recorded in order to investigate the cell performance by assembling two Toray GDLs. The cell temperature was 80 °C, the H_2 and O_2 pressure was 2.5 bar(abs) and the humidifier temperature was set to 85 °C. Compared to a commercial MEA from Paxitec with 0.4 mg Pt cm^{-2} loading, the inkjet printed MEA from LEPA not only has a lower Pt loading, but also shows higher ohmic losses. However, as it has been demonstrated recently inkjet printing can compete with other MEA fabrication techniques after ink and process optimization.

Recently, LEPA has started to develop approaches to fabricate a complete MEA including 2 CLs and the polymer electrolyte membrane by inkjet printing on a Nafion NR-212 support (Fig. 4a). 60 IJPLs of the Pt/C-Nafion ink, 30 IJPLs of the Nafion ink and again 60 IJPLs of the Pt/C-Nafion ink were deposited and can

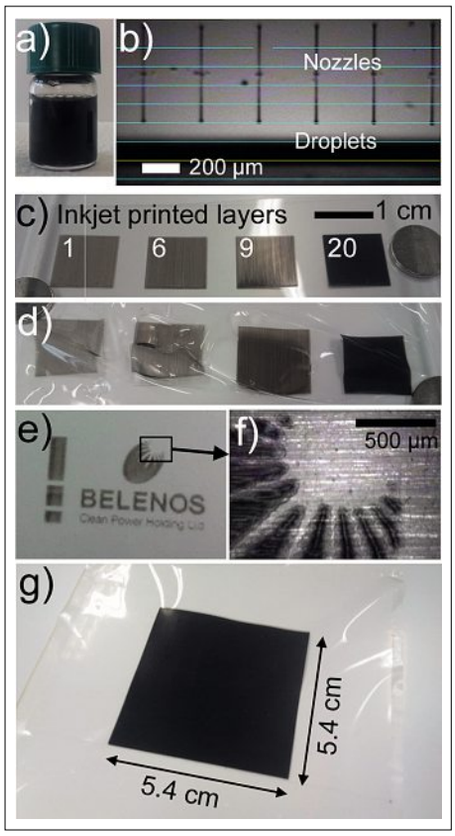

Fig. 3. Inkjet printing of Pt/C-Nafion ink on Nafion NR 212 membrane (CCM principle). a) Formulated Pt/C-Nafion ink. b) Stable jetting with 6 exemplary consecutive nozzles. c) 1 cm × 1 cm CLs made by various IJPLs. d) Samples from (c) after immersion test in DI water at 60°C for 12 h. e) High resolution inkjet printing of the Pt/C-Nafion ink. f) Zoom of (e). g) Inkjet printed MEA (5.4 cm × 5.4 cm) composed of a commercial Nafion NR-212 membrane enclosed by two printed CLs each made of 30 IJPLs.

be clearly identified by HR SEM as shown for the cross-section in Fig. 4b. The Nafion inter-layer shows a similar compactness to the Nafion support. The two CLs look identical and an accumulation of catalyst NPs can clearly be seen. HR SEM allowed the determination of the thickness of the Pt/C based CL to be about 6 µm while the Nafion membrane layer inbetween the two CLs was about 6.5 µm thick (Fig. 4c). These results demonstrate the possibility to prepare consecutively all three layers of a MEA by inkjet printing. In future studies, the stability and functionality of the fully inkjet printed MEA will be investigated and the fabrication process optimized (*e.g.* layer thickness, catalyst loading, post-processing and removal from the support).

Consequently, inkjet printing should enable to print a complete MEA directly onto a GDL, such as Toray paper. A second GDL would then be pressed on top. Inkjet printing of a complete MEA onto a GDL is principally possible (Fig. 5a), as reported previously by Taylor *et al.*,[37] but it suffers clearly from the porosity of the GDL. A main part of the ink goes inside the Toray paper rather than staying on the top of the three-dimensional carbon fiber network (Fig. 5b and c). As a result, the ink can run several tens of micrometers into the carbon fiber network. To overcome such an issue, a less porous GDL could be employed, the empty space of the GDL could temporarily be filled by another material and/or the hydrophobic properties of the GDL could be adjusted to keep the printed inks on the top and thus forming compact layers.

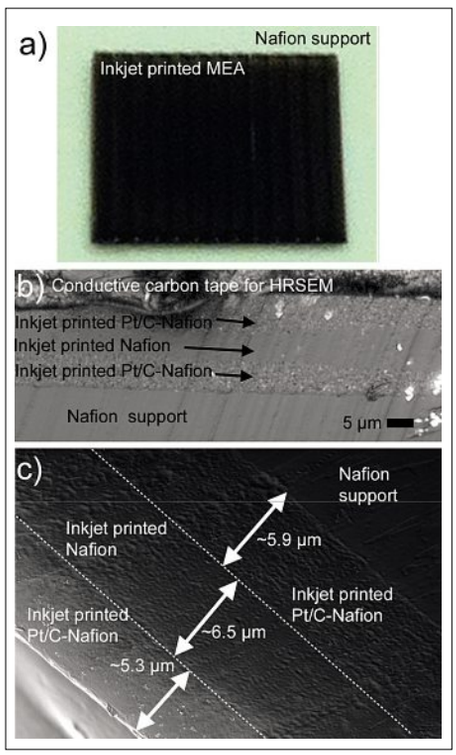

Fig. 4. Fully inkjet printed 5 mm × 5 mm MEA composed of 60 IJPLs of Pt/C-Nafion ink, 30 IJPLs Nafion ink and 60 IJPLs of Pt/C-Nafion ink on a Nafion NR 212 support. a) Photograph showing the top view. b) Laser scanning micrograph and c) HR SEM of the cross-section.

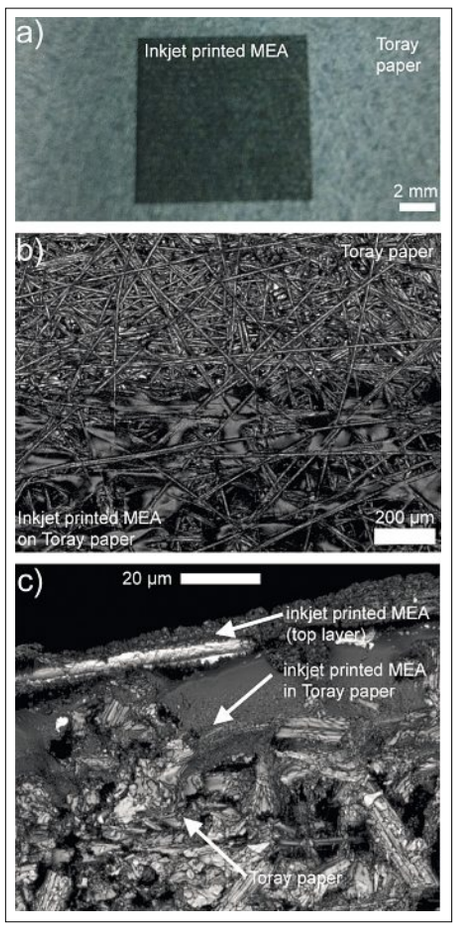

Fig. 5. Inkjet printing of a MEA on a standard Toray GDL (CCG principle). a) Optical photograph of an inkjet printed MEA of 10 mm × 10 mm CL (60 IJPLs of Pt/C-Nafion ink, 30 IJPLs Nafion ink and 60 IJPLs of Pt/C-Nafion ink). Laser scanning micrographs showing a) the top view on the border between bare GDL and GDL coated with the MEA layers and c) the cross-section of the GDL coated with MEA layers.

4. Conclusion and Outlook

Inkjet printing has demonstrated its potential for many applications including electrochemical energy conversion, although it has not yet reached standard industrial production for functional materials. The main issues are the ink properties, the jetting parameters, the ink–substrate interaction and the post-processing step. Nowadays, many solutions for inkjet printing in terms of printheads and printing devices are provided by a growing number of manufacturers. The printhead technology is further developed, but also the operating systems become more powerful and more flexible in terms of software and integrated post processing techniques such as UV, NIR and photonic curing. Recently, LEPA has purchased a Ceradrop X-Serie inkjet printer with three printheads, simultaneous UV curing option and an integrated PulseForge 1300 photonic curing post processing station from Novacentrix (Fig. 6). Such a system allows sequential and quasi-simultaneous printing of various materials to obtain material gradients and multilayers completed by curing in one fabrication process without removing the substrate in-between layer fabrication. This very powerful system is currently unique worldwide and dedicated among other applications to print precious and low cost electrocatalysts, combinatorial

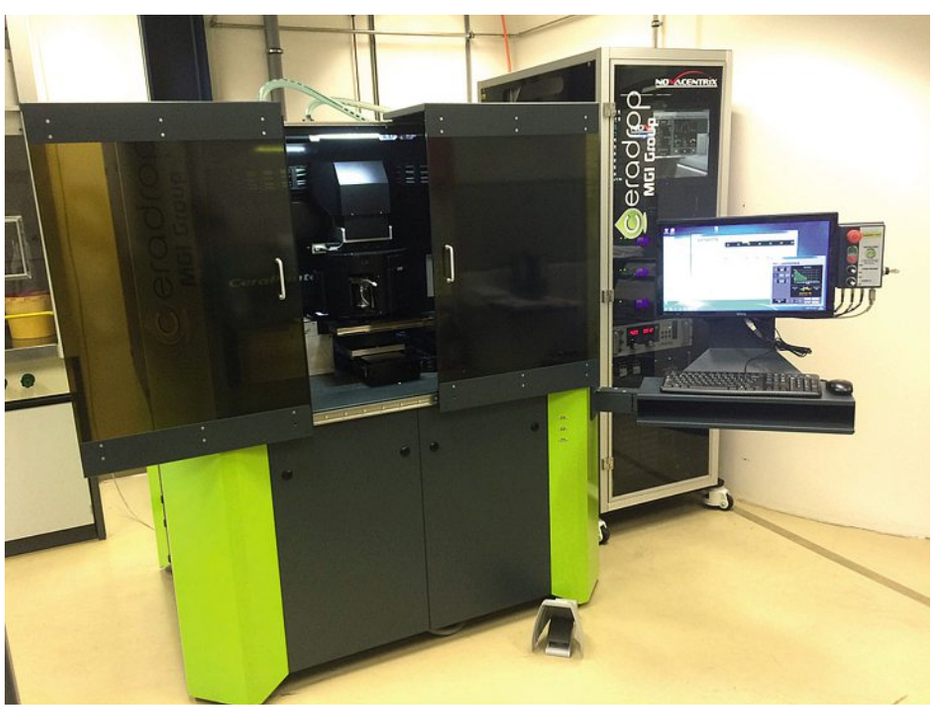

Fig. 6. In the new EPFL campus 'Energypolis' in Sion, LEPA employs an X-Serie inkjet printer from Ceradrop with three printheads and an integrated PulseForge 1300 photonic curing station.

libraries, catalyst layers and electrolyte membranes for energy conversion devices such as fuel cells, redox flow batteries and metal air batteries.

5. Experimental

5.1 *Materials*

Carbon-supported Pt HiSPEC 9100 was purchased from Johnson Matthey Fuel Cells and contains 57 to 61 wt% of Pt. Nafion NR-212 membranes were obtained from IonPower. Toray Carbon Paper (TGP-H-090 10% Wet Proofing) was used as GDL and shows increased hydrophobic properties due to a Teflon treatment. Nafion ionomer (D250, 1000 EW, 5%, Ion Power) and isopropanol (Merck Milipore) were used as received. Deionized (DI) water was produced by a Milli-Q plus 185 model (Merck Millipore).

5.2 *Ink Formulation*

The ink for inkjet printing of the catalyst layer was prepared by adding HiSPEC 9100 after slight oxygen plasma treatment to introduce some hydrophilic groups on the NP surface to DI water. After an ultrasound treatment using either an ultrasonic bath or an Ultrasonics Processor Type VC 505 with 3 mm Stepped Micro Tip (Sonics), sufficient amounts of the Nafion ionomer solution and isopropanol were added. After a second sonication step and continuous agitation, particle aggregates, which were not broken by sonication, were separated by centrifugation for 2 min at 10,000 rpm. The surface tension and viscosity of the ink were 25.7 mN m^{-1} and 4.1 mPas, respectively. A Nafion-based ink was obtained by adding to the Nafion ionomer solution subsequently isopropanol and DI water resulting in an ink with a surface tension of 26.5 mN m^{-1} and a viscosity of 8.2 mPas. Both prepared inks were homogeneous and stable during the entire printing processes. The surface tension was measured using a Drop Shape Analyzer DSA100 (Krüss) and the viscosity was determined with a SV-1A series viscometer (AandD).

5.3 *Inkjet Printing*

For inkjet printing of the CLs and the polymer electrolyte membrane the drop-on-demand Dimatix materials printer DMP-2831 and disposable cartridges with piezoelectric-based nozzles generating 10 pL nominal droplet volumes were used (Dimatix Fujifilm). The cartridge contains 16 nozzles from which between 6 and 16 could be used in the present work. All printing parameters such as waveform, jetting frequency, nozzle height and drop spacing were optimized for each ink. The substrate temperature was generally increased to 50 or 60 °C in order to enhance the evaporation rate of the ink solvents during printing. After the printing process, curing of the printed patterns was performed by a thermal treatment at 80 °C for 30 min with a heating and cooling rate of 1 °C min^{-1}.

5.4 *MEA Characterization*

The printed patterns were investigated using laser scanning microscopy in reflection mode with a Keyence VK 8700 (Keyence) and high-resolution scanning electron microscopy (HR SEM) using a SEM MERLIN composed of a GEMINI II column (Zeiss). Cross-sections of the printed layers were obtained by razor blade cutting. Energy dispersive X-ray fluorescence microscopy analysis was performed to determine the Pt loading in the CLs.

Acknowledgements

The work was supported by the Swiss Commission for Technology and Innovation (CTI, project No. 13999.2) and the Swiss Competence Center for Energy Research SCCER Heat and Energy Storage. A.L. and V.C.B. thank the Swiss National Science Foundation (SNSF project No. 154297). Dr. Elli Varkaraki and Dr. José-Antonio Gonzalez from Belenos Clean Power Holding Ltd. (Switzerland) are thanked for the collaborative work on the development of the inkjet printed MEAs. Jürg Thut and Dr. Lorenz Gubler from the Paul Scherrer Institute (PSI, Switzerland) are thanked for testing the inkjet printed and commercial MEAs. The Center of Micronanotechnology (CMi) at the EPFL is acknowledged for the access to the Dimatix DMP-2831 printer and the technical support. Prof. Dr. Kevin Sivula (EPFL) is thanked for providing the drop shape analyzer to measure the surface tension of the inks.

Received: February 28, 2015

[1] P. Calvert, *Chem. Mater.* **2001**, *13*, 3299.
[2] B. J. De Gans, P. C. Duineveld, U. S. Schubert, *Adv. Mater.* **2004**, *16*, 203.
[3] A. Kamyshny, S. Magdassi, *Small* **2014**, *10*, 3515.
[4] M. Singh, H. M. Haverinen, P. Dhagat, G. E. Jabbour, *Adv. Mater.* **2010**, *22*, 673.
[5] T. Boland, T. Xu, B. Damon, X. Cui, *Biotech. J.* **2006**, *1*, 910.
[6] Y. Xu, I. Hennig, D. Freyberg, A. J. Strudwick, M. G. Schwab, T. Weitz, K. C. Cha, *J. Power Sources* **2014**, *248*, 483.
[7] G. D. Martin, S. D. Hoath, I. M. Hutchings, *J. Phys.: Conf. Ser.* **2008**, *105*, 012001.
[8] J.-U. Park, M. Hardy, S. J. Kang, K. Barton, K. Adair, D. K. Mukhopadhyay, C. Y. Lee, M. S. Strano, A. G. Alleyne, J. G. Georgiadis, P. M. Ferreira, J. A. Rogers, *Nat. Mater.* **2007**, *6*, 782.
[9] S. Mishra, K. L. Barton, A. G. Alleyne, P. M. Ferreira, J. A. Rogers, *J. Micromech. Microeng.* **2010**, *20*, 095026.
[10] E. Sutanto, K. Shigeta, Y. K. Kim, P. G. Graf, D. J. Hoelzle, K. L. Barton, A. G. Alleyne, P. M. Ferreira, J. A. Rogers, *J. Micromech. Microeng.* **2012**, *22*, 045008.
[11] P. Galliker, J. Schneider, H. Eghlidi, S. Kress, V. Sandoghdar, D. Poulikakos, *Nat. Commun.* **2012**, *3*, 890.
[12] B. Derby, *Annu. Rev. Mater. Res.* **2010**, *40*, 395.
[13] H. Wijshoff, *Phys. Rep.* **2010**, *491*, 77.
[14] D. Soltman, V. Subramanian, *Langmuir* **2008**, *24*, 2224.
[15] E. B. Duoss, M. Twardowski, J. A. Lewis, *Adv. Mater.* **2007**, *19*, 3485.
[16] M. Kuang, L. Wang, Y. Song, *Adv. Mater.* **2014**, *26*, 6950.
[17] E. Reddington, A. Sapienza, B. Gurau, R. Viswanathan, S. Sarangapani, E. S. Smotkin, T. E. Mallouk, *Science* **1998**, *280*, 1735.
[18] S. Guerin, B. E. Hayden, D. Pletcher, M. E. Rendall, J. P. Suchsland, *J. Comb. Chem.* **2006**, *8*, 679.
[19] E. S. Smotkin, J. Jiang, A. Nayar, R. Liu, *Appl. Surf. Sci.* **2006**, *252*, 2573.
[20] J. L. Fernández, D. A. Walsh, J. A. Bard, *J. Am. Chem. Soc.* **2005**, *127*, 357.
[21] J. L. Fernández, V. Raghuveer, A. Manthiram, A. J. Bard, *J. Am. Chem. Soc.* **2005**, *127*, 13100.
[22] J. M. Gregoire, C. Xiang, X. Liu, M. Marcin, J. Jin, *Rev. Sci. Instrum.* **2013**, *84*, 024102.
[23] J. L. Fernández, A. J. Bard, *Anal. Chem.* **2003**, *75*, 2967.
[24] D. Seley, K. Ayers, B. A. Parkinson, *ACS Comb. Sci.* **2013**, *15*, 82.
[25] X. Liu, T.-J. Tarn, F. Huang, J. Fan, *Particuology*, **2015**, *19*, 1.
[26] M. Woodhouse, G. S. Herman, B. A. Parkinson, *Chem. Mater.* **2005**, *17*, 4318.
[27] M. Woodhouse, B. A. Parkinson, *Chem. Soc. Rev.* **2009**, *38*, 197.
[28] J. He, B. A. Parkinson, *ACS Comb. Sci.* **2011**, *13*, 399.
[29] C. Jiang, R. Wang, B. A. Parkinson, *ACS Comb. Sci.* **2013**, *15*, 639.
[30] M. Woodhouse, B. A. Parkinson, *Chem. Mater.* **2008**, *20*, 2495.
[31] J. E. Katz, T. R. Gingrich, E. A. Santori, N. S. Lewis, *Energy Environ. Sci.* **2009**, *2*, 103.
[32] X. Liu, Y. Shen, R. Yang, S. Zou, X. Ji, L. Shi, Y. Zhang, D. Liu, L. Xiao, X. Zheng, S. Li, J. Fan, G. D. Stucky, *Nano Letters* **2012**, *12*, 5733.
[33] J. M. Gregoire, C. Xiang, S. Mitrovic, X. Liu, M. Marcin, E. W. Cornell, J. Fan, J. Jin, *J. Electrochem. Soc.* **2013**, *160*, F337.
[34] J. A. Haber, Y. Cai, S. Jung, C. Xiang, S. Mitrovic, J. Jin, A. T. Bell, J. M. Gregoire, *Energy Environ. Sci.* **2014**, *7*, 682.
[35] A. Shinde, D. Guevarra, J. A. Haber, J. Jin, J. M. Gregoire, *J. Mater. Res*. **2015**, *30*, 442.
[36] C. Xiang, S. K. Suram, J. A. Haber, D. W. Guevarra, E. Soedarmadji, J. Jin, J. M. Gregoire, *ACS Comb. Sci.* **2014**, *16*, 47.
[37] A. D. Taylor, E. Y. Kim, V. P. Humes, J. Kizuka, L. T. Thompson, *J. Power Sources* **2007**, *171*, 101.
[38] S. Towne, V. Viswanathan, J. Holbery, P. Rieke, *J. Power Sources* **2007**, *171*, 575.
[39] M. S. Saha, D. Malevich, E. Halliop, J. G. Pharoah, B. A. Peppley, K. Karan, *J. Electrochem. Soc.* **2011**, *158*, B562.
[40] S. Shukla, K. Domican, K. Karan, S. Bhattacharjee, M. Secanell, *Electrochim. Acta* **2015**, *156*, 289.
[41] M. Yazdanpour, A. Esmaeilifar, S. Rowshanzamir, *Int. J. Hydrogen Energy* **2012**, *37*, 11290.
[42] Z. Wang, Y. Nagao, *Electrochim. Acta* **2014**, *129*, 343.
[43] A. Lesch, F. Cortés-Salazar, M. Prudent, J. Delobel, S. Rastgar, N. Lion, J.-D. Tissot, P. Tacchini, H. H. Girault, *J. Electroanal. Chem.* **2014**, *717*, 61.
[44] A. Lesch, F. Cortés-Salazar, V. Amstutz, P. Tacchini, H. H. Girault, *Anal. Chem.* **2015**, *87*, 1026.
[45] A. Lesch, P.-C. Chen, F. Roelfs, C. Dosche, D. Momotenko, F. Cortés-Salazar, H. H. Girault, G. Wittstock, *Anal. Chem.* **2013**, *86*, 713.
[46] L. Qiao, E. Tobolkina, A. Lesch, A. Bondarenko, X. Zhong, B. Liu, H. Pick, H. Vogel, H. H. Girault, *Anal. Chem.* **2014**, *86*, 2033.